On equations for bent thin-wire antennas

Alexander G. Voronovich, Paul E. Johnston, *Life Member IEEE,* Richard J. Lataitis, *Life Senior Member, IEEE*

***Abstract*—The Pocklington equation in its standard form can be considered a Fredholm integral equation of the first kind with a singular kernel. Managing the singularity during numerical simulations presents certain practical difficulties. In this paper, an alternative form of the Pocklington equation for a thin, bent, ideally conducting wire is derived in the form of a Fredholm integral equation of the second kind with a regular kernel, which is better suited for numerical treatment. The kernel of the integral equation does not depend on the wire radius, which enters only through diagonal elements of the interaction matrix. Both cases of loop and open-ended wires are considered with loop wire antennas allowing for a particularly simple formulation. Numerical simulations confirm the validity of the derived equations. Numerical results calculated for a specific circular loop antenna match available experimental data.**

***Index Terms*—Thin wire antennas, ideal conductors, the Pocklington equation.**

I. Introduction

Classical integral or integral-differential equations of the Pocklington and Hallen type [1,2], describing radiation and scattering of EM fields by thin, ideally conducting wires, are of significant practical interest and have been extensively studied. These equations follow from the boundary condition that requires absence of the tangential component of the total electric field at the wire surface. The total electric field consists of both a known incident and scattered field, the latter due to a generally unknown current induced in the wire. The scattered electric field at a given point on the wire surface consists both of a "far" field associated with observation points separated from a given point on the wire by distances significantly exceeding the wire's radius a, and by a "near" field associated with nearby observation points that can be arbitrarily close to a given point on the wire. Near field calculations require managing a logarithmic singularity in the kernel of the Pocklington equation. This singularity is an important feature that makes the Pocklington equation solvable and well-posed [3,4]. This singularity can be avoided by replacing the boundary condition at the wire's surface by the requirement that the electric field vanish at the central core of the wire, since the total electric field inside an ideally conducting wire must also tend to zero. Such a replacement, however, renders the resulting equation, strictly speaking, non-solvable [5,6]. Moreover, such a replacement does not eliminate the necessity of an accurate treatment of the near field, which has a significantly different structure that the far field.

Numerical solutions of the thin wire equations are usually obtained with the help of the method of moments (see, e.g. [2], or many other textbooks dealing with antenna theory). In this case the problem generally reduces to calculation of integrals of products of the kernel, and basis and trial functions selected for numerical solution. The "exact" kernel of the Pocklington equation can be generally expressed in terms of elliptic functions, and the calculation of the corresponding integrals may be nontrivial and time consuming (see, e.g., [7-9]). The ultimate source of these complexities is the presence of the near field. Calculations of contributions from the far field are straightforward. There is, however, no distinct boundary separating the near and far fields.

Most of the published work on wire antennas considers the case of straight wires. Bent wires were first considered in [10-12]. Concrete applications for the case of an elliptical wire have also been presented (e.g., in [13]). In this development an approximate kernel was used, and the near field calculation was treated numerically. The issues associated with singularities of the kernels in the integral equations pertain to both straight and bent wires.

For the reasons outlined above, the representation of the Pocklington equation in a form where the effects of the near field are extracted and treated analytically, and the remaining kernel of the integral term is rendered non-singular (including the limit $a \to 0$), is of interest. One possibility to achieve this is to subtract from the kernel the corresponding logarithmic term [14]. However, this makes the governing equation more cumbersome because the logarithmic term, correctly describing the interaction of currents at small distances, is inaccurate at larger distances, and the corresponding contributions must be compensated.

In this paper an alternative approach for handling the singularity in the kernel of the Pocklington equation is suggested. Namely, we demonstrate that the contribution from the near field can be represented as a sum of two terms: an integral with a wire-radius-independent, non-singular kernel, and a second term in the form of a scalar factor that contains the Hankel function with the argument proportional to the wire radius. Thus, the Pocklington equation, which in its traditional

This paragraph of the first footnote will contain the date on which you submitted your paper for review. It will also contain support information, including sponsor and financial support acknowledgment. For example, "This work was supported in part by the U.S. Department of Commerce under Grant BS123456."

A.G. Voronovich, P.E. Johnston, and R.J. Lataitis are with the NOAA Physical Sciences Laboratory, 325 Broadway, Boulder, CO, 80305. P.E. Johnston is also with University of Colorado Cooperative Institute for Research in the Environmental Sciences, and R.J. Lataitis with the Science and Technology Corporation.

form represents a Fredholm integral equation of the first kind with a singular kernel, becomes essentially a Fredholm integral equation of the second kind with a non-singular kernel. An additional useful feature of the new representation is that the non-singular kernel does not depend on the wire radius. Both cases of a loop and open-ended wire antenna are considered. The case for the loop antennas allows for a particularly simple formulation.

II. Derivation

The derivation that follows is somewhat lengthy. Before proceeding we outline the major logical steps. First, we specify a general equation representing an electric field in terms of a current density for the case of a thin-wire and substitute the corresponding expression into the boundary condition. The boundary condition assumes an ideal conductor and is formulated as a limit when an observation point tends to the surface of the wire (eqs. (1) – (5)). Second, to facilitate calculation of the limit we divide the wire into two parts: the points separated from the observation point by a distance Δs that significantly exceeds radius of the wire a (i.e., the "far" points responsible for the "far" field), and the points that can be arbitrarily close to the observation point (i.e., the "near" points responsible for the "near" field (see eqs. (6)-(7)). Third, we represent the current along the wire as a superposition of harmonics (eqs. (8)-(15)) and consider the contribution from each harmonic separately. The calculation of the far field contribution is straightforward, however, the contribution from the near field requires a bit of extra work. Thus, at the fourth step, we approximate a piece of the wire in the vicinity of the observation point by a section of a straight cylinder and calculate the near field by extending the section of the cylinder to infinity and subtracting the contribution from the added "wings" (eqs. (16)-(17)). The contribution from the infinite cylinder is calculated using a well-known integral that leads to an explicit formula where the limit can be calculated by a direct substitution (eqs. (17)-(18)). Finally, combining all terms yields our resulting eq. (23). The geometry and some notations are illustrated in Fig.1.

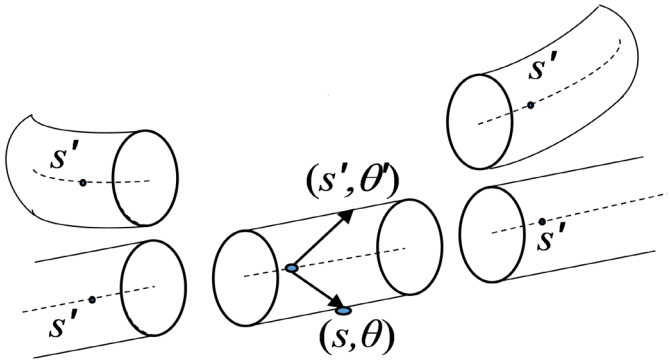

Fig. 1: Illustration of the geometry and the field calculation procedure. A section of the wire approximated by a small section of a straight cylinder is shown in the center. The imaginary "wings" due to the extension of the straight section to infinity are shown to the left and right. For easier rendering, the rest of the curved wire beyond the central piece, which represent the imaginary "wings", is shifted upwards. Here (s,θ) and (s',θ') define, respectively, the observation point and the contributing "near-field" (central section) and "far-field" (wings) points at the wire surface, where s, s' describe arc lengths along the wire axis, and θ, θ' azimuthal points on the wire surface.

Maxwell's equations for a monochromatic wave of frequency ω propagating in free space are given by:

$$\nabla\times\vec{H}=\tilde{\vec{j}}-i\omega\varepsilon_0\vec{E},\ \nabla\times\vec{E}=i\varepsilon\mu_0\vec{H},\ \nabla\cdot\vec{E}=\rho/\varepsilon_0,\quad (1a)$$

where a time dependence $exp(-i\omega t)$ is assumed, and $\tilde{\vec{j}}$ and ϱ represent the current and charge densities, respectively. Applying the $\nabla\times$ operator to the second equation in (1a) above one obtains:

$$\left(\nabla^2+K^2\right)\vec{E}=-\frac{i}{\varepsilon_0\omega}\left(K^2\tilde{\vec{j}}+\nabla\left(\nabla\cdot\tilde{\vec{j}}\right)\right),\qquad (1b)$$

where $K=\omega/c$ is a wavenumber and the equation for the conservation of charge $i\omega\varrho=\nabla\tilde{j}$ was also used. From (1b) the n-th component ($n = 1,2,3$) of the electric field at a point $\vec{R}$ due to the currents $\tilde{\vec{j}}$ (which we refer to as a scattered field) in index notation is given by

$$E_n^{(sc)}\left(\vec{R}\right)=\frac{i}{4\pi\varepsilon_0\omega}\int\left(\begin{array}{c}K^2g\left(\vec{R}-\vec{R}'\right)\tilde{j}_n\left(\vec{R}'\right)-\\ -\frac{\partial^2 g\left(\vec{R}-\vec{R}'\right)}{\partial x_n\partial x'_\alpha}\tilde{j}_\alpha\left(\vec{R}'\right)\end{array}\right)dV_{\vec{R}'},\qquad (2)$$

where

$$g\left(\vec{R}\right)=\frac{e^{iKr}}{r},\quad r=\left|\vec{R}\right|$$

coincides with the Green's function for the wave equation in 3D within a factor of $-1/(4\pi)$.

The boundary condition for an ideal conductor is given by:

$$\vec{\tau}\left(\vec{E}^{(sc)}\left(\vec{R}\right)+\vec{E}^{(in)}\left(\vec{R}\right)\right)_{\vec{R}\in\Sigma}=0,\qquad (3)$$

where $\vec{\tau}$ is an arbitrary vector tangent to the surface Σ of the ideal conductor and $\vec{E}^{(in)}$ is an incident electric field. Let us consider the case of a thin wire:

$$Ka>>1,$$

where a is the radius of the wire. Let s be an arc length calculated along the central line of the wire. We will assume that the skin-layer depth is very small so that the volume integration in (2) reduces to a surface integration. According to the thin wire approximation we will assume that the current at a given cross-section of the wire is uniformly distributed over the wire circumference and is directed along the axis of the wire. Then

$$\tilde{\vec{j}}\left(\vec{R}\right)=\frac{j_s}{2\pi a}\frac{d\vec{r}_s}{ds},\qquad (4)$$

where j_s is a total current at a wire's cross-section at a point

s and $\vec{r}_s = \vec{r}(s)$ are coordinates of the center line at point s. Substituting (4) into (2), and the result into the boundary condition (3), and setting in (3) $\vec{\tau} = d\vec{r}_s/ds$ we represent the boundary condition in the following form:

$$\lim_{\vec{R}\to\vec{\rho}(s,\theta)} \int \left(K^2 g\left(\vec{R}-\vec{R}'\right)\frac{dr_n}{ds}\frac{dr'_n}{ds'} - \frac{\partial^2 g\left(\vec{R}-\vec{R}'\right)}{\partial x_n \partial x'_\alpha}\frac{dr_n}{ds}\frac{dr'_\alpha}{ds'} \right)_{\vec{R}'=\vec{\rho}(s',\theta')} \times j_{s'}\frac{d\theta'}{2\pi}ds' = i4\pi\omega\varepsilon_0 \vec{E}^{(in)}\left(\vec{r}_s\right)\frac{d\vec{r}_s}{ds}, \tag{5}$$

where θ, θ' are azimuthal angles at the cross-section planes of the wire at points s, s', correspondingly, and the points $\vec{\rho}(s,\theta)$ and $\vec{\rho}(s',\theta')$ describe the wire surface. We put in the LHS of (5) a limit sign since if one immediately sets $\vec{R} = \vec{\rho}(s,\theta)$ the integral will generally contain non-integrable singularities (due to $|\vec{R}-\vec{R}'|^{-2,-3}$ order terms).

To facilitate calculation of the limit we will split the integration over s' in (5) into an integration over far points s' that are separated from the point s by some finite interval Δs with $|s'-s|>\Delta s$ and near points with $|s'-s|<\Delta s$. We will assume that the selected half-length of the interval Δs significantly exceeds the radius of the wire a but is significantly smaller than characteristic radius of curvature c_{wire}^{-1} of the central line of the wire, that is, $a \ll \Delta s \ll c_{wire}^{-1}$. With respect to the far points in the RHS of (5) to an accuracy of $O(Ka)$ one can set $\vec{R} = \vec{r}_s$ and $\vec{R}' = \vec{r}_{s'}$. With respect to the near points we will approximate the corresponding piece of wire by a straight cylinder. Let us assume that the observation point $\vec{R}$ tends to the point $\vec{\rho}(s,\theta)$ on the wire surface along the ray that is orthogonal to the central line of the wire at a point s and has azimuthal angle θ. In this case for the near points one has:

$$D = \left|\vec{R}-\vec{R}'\right| = \left[b^2 + a^2 - 2ab\cos\left(\theta-\theta'\right) + \left(s-s'\right)^2\right]^{1/2},$$

where D is the distance between the observation point and a point $\vec{\rho}(s',\theta')$ on the straight cylinder surface and $b = |\vec{R}-\vec{r}_s|$ is the distance between the observation point and the wire's central line. Performing a straightforward calculation for the far points one can write (5) as:

$$\lim_{b\to a}\int_0^{2\pi}\frac{d\theta'}{2\pi}\int_{s-\Delta s}^{s+\Delta s}\left(K^2 g(D)\left(\frac{d\vec{r}}{ds},\frac{d\vec{r}'}{ds'}\right) - \frac{\partial^2 g(D)}{\partial s\partial s'}\right) j_{s'}ds' + \int_{|s-s'|>\Delta s} U(s,s')\, j_{s'}ds' = i4\pi\varepsilon_0\omega\vec{E}^{(in)}\left(\vec{r}_s\right)\frac{d\vec{r}_s}{ds}, \tag{6}$$

where

$$U(s,s') = \frac{e^{iKr}}{r^3}\left[\left(K^2r^2 + iKr - 1\right)\left(\frac{d\vec{r}_s}{ds},\frac{d\vec{r}_{s'}}{ds'}\right) - \left(K^2r^2 + 3iKr - 3\right)\left(\frac{\vec{r}_s-\vec{r}_{s'}}{r},\frac{d\vec{r}_s}{ds}\right)\left(\frac{\vec{r}_s-\vec{r}_{s'}}{r},\frac{d\vec{r}_{s'}}{ds'}\right)\right]_{r=|\vec{r}_s-\vec{r}_{s'}|}. \tag{7}$$

Note that U in (7) is a symmetric function $U(s,s') = U(s',s)$. Let us represent j_s as a superposition of the Fourier harmonics:

$$j_s = \int_{-\infty}^{\infty} e^{ips} j_p dp, \tag{8}$$

where spectral parameter p has a dimension of wavenumber. Now we represent (6) as follows:

$$\int_{-\infty}^{\infty} L_p(s)\,\hat{j}_p dp = i4\pi\varepsilon_0\omega\vec{E}^{(in)}\left(\vec{r}_s\right)\frac{d\vec{r}_s}{ds}, \tag{9}$$

where

$$L_p(s) = \lim_{b\to a}\int_0^{2\pi}\int_{s-\Delta s}^{s+\Delta s}\left(K^2 g(D)\left(\frac{d\vec{r}}{ds},\frac{d\vec{r}'}{ds'}\right) - \frac{\partial^2 g(D)}{\partial s\partial s'}\right) e^{ips'}ds'\frac{d\theta'}{2\pi} + \int_{|s-s'|>\Delta s} U(s,s')e^{ips'}ds'. \tag{10}$$

Integrating by parts we obtain:

$$\int_{s-\Delta s}^{s+\Delta s}\frac{\partial^2 g(D)}{\partial s\partial s'}e^{ips'}ds' = \left(ipg(D) - \frac{\partial g(D)}{\partial s'}\right)e^{ips'}\Big|_{s'=s-\Delta s}^{s'=s+\Delta s} + p^2\int_{s-\Delta s}^{s+\Delta s} g(D)e^{ips'}ds'. \tag{11}$$

When calculating substitutions in (11) we take into account the condition $\Delta s \gg a$ and approximate

$$g(D) \approx \frac{e^{iK|s-s'|}}{|s-s'|}. \tag{12}$$

Then straightforward calculations give:

$$\left(ipg(D) - \frac{\partial g(D)}{\partial s'}\right)e^{ips'}\Big|_{s'=s-\Delta s}^{s'=s+\Delta s} = 2e^{ips+iK\Delta s}\left[\left[\frac{iK\Delta s - 1}{(\Delta s)^2}\cos(p\Delta s) + \frac{p}{\Delta s}\cdot\sin(p\Delta s)\right]\right] = e^{ips}\int_{|t|>\Delta s}\left(-\frac{2}{|t|^3} + \frac{2iK}{t^2}\right)e^{iK|t|+ipt}dt + 2e^{ips}K_p^2\int_{\Delta s}^{\infty}\frac{e^{iKt}}{t}\cos ptdt, \tag{13}$$

where

$$K_p = \sqrt{K^2 - p^2}, \quad \mathrm{Im}\,K_p \geq 0. \tag{14}$$

One can easily check the integral representation of the middle expression in (13) by differentiation with respect to Δs. Now (10) becomes:

$$L_p(s)=\lim_{b\to a}K_p^2\int_0^{2\pi}\int_{s-\Delta s}^{s+\Delta s}g(D)e^{ips'}ds'\frac{d\theta'}{2\pi}+2e^{ips}K_p^2\int_{\Delta s}^{\infty}\frac{e^{iKt}}{t}\cos ptdt \qquad (15)$$
$$+e^{ips}\int_{|t|>\Delta s}\left(-\frac{2}{|t|^3}+\frac{2iK}{t^2}\right)e^{iK|t|+ipt}dt+\int_{|s-s'|>\Delta s}U(s,s')e^{ips'}ds'.$$

To calculate in the RHS of (15) in the limit $b\to a$ we first extend the integration over s' to infinite limits and then subtract from the result the contribution from points $|s\text{-}s'|>\Delta s$. Again, for the "far" points approximation (12) can be used, and one finds:

$$\int_{s-\Delta s}^{s+\Delta s}g(D)e^{ips'}ds'=\int_{-\infty}^{\infty}g(D)e^{ips'}ds'-2e^{ips}\int_{\Delta s}^{\infty}\frac{e^{iKt}}{t}\cos ptdt. \qquad (16)$$

Using formula 3.876 (1,2) from [15] one obtains:

$$\int_{-\infty}^{\infty}g(D)e^{ips'}ds'=\int_{-\infty}^{\infty}\frac{\exp\left(iK\sqrt{d^2+(s-s')^2}\right)}{\sqrt{d^2+(s-s')^2}}e^{ips'}ds'=i\pi e^{ips}H_0^{(1)}(K_pd), \qquad (17)$$

where

$$d^2=b^2+a^2-2ab\cos(\theta-\theta').$$

When one crosses the surface of the cylinder the tangent electric field remains continuous, and it does not matter whether we calculate the limit $b\to a$ from inside or outside of the cylinder. Let us assume that the observation point approaches the cylinder surface from inside of the cylinder (which we thus consider a "hollow tube"). Integration of the RHS of (17) over θ' is closely associated with the problem of diffraction of EM waves from an infinite, perfectly conducting cylinder, and it can be evaluated using formula 8.531(2) from [15]:

$$\int_0^{2\pi}H_0^{(1)}\left(K_p\sqrt{b^2+a^2-2ab\cos(\theta-\theta')}\right)\frac{d\theta'}{2\pi}= \qquad (18)$$
$$=H_0^{(1)}(K_pb)J_0(K_pa).$$

Now the limit $b\to a$ can be calculated by simply setting in the RHS of (18) $b=a$. Substituting (16) and (18) into (15) one obtains:

$$L_p(s)=i\pi K_p^2e^{ips}H_0^{(1)}(K_pa)J_0(K_pa)+ \qquad (19)$$
$$+e^{ips}\int_{|t|>\Delta s}\left(-\frac{2}{|t|^3}+\frac{2iK}{t^2}\right)e^{iK|t|+ipt}dt+\int_{|s-s'|>\Delta s}U(s,s')e^{ips'}ds',$$

or, after replacing in the first integral in the RHS of (19) $t=s'-s$:

$$L_p(s)=i\pi K_p^2e^{ips}H_0^{(1)}(K_pa)J_0(K_pa)+ \qquad (20)$$
$$+K^3\int_{|s-s'|>\Delta s}V(s,s')e^{ips'}ds'$$

where

$$K^3V(s,s')=\left(-\frac{2}{|s'-s|^3}+\frac{2iK}{(s'-s)^2}\right)e^{iK|s'-s|}+U(s,s'). \qquad (21)$$

We note one important point here. After multiplication by $\hat{j}_p$ and integration over p according to (8), both the second and third terms in the RHS of (19) become integrals over ds' with the integrands proportional to $j_{s'}$. For this reason, for an open-ended antenna, the integration over s' should proceed over the length of the antenna only since $j_{s'}$ becomes zero beyond it. This fact is used in (24) below. For a loop antenna, however, this is not true, since in this case $j_{s'}$ becomes a periodic function of s', and the contribution from s' lying beyond $(-L/2, L/2)$ has to be subtracted from the second term in (19) (see equation (29) in the next Section).

Normalization by K^3 introduced in (21) makes $V(s,s')$ dimensionless. It is also a symmetric function:

$$V(s,s')=V(s',s). \qquad (22)$$

It is demonstrated in Appendix A that the function $V(s,s')$ is continuous at $s=s'$ since singularities in the parentheses and U-term in (21) cancel out. This fact represents the major finding of this work. It confirms indirectly that approximation of the piece of wire at $|s-s'|<\Delta s$ by a straight cylinder is sufficient and a more accurate approximation is not needed. Due to the regularity of $V(s,s')$ at $s=s'$ we can now extend the integration over s' in the second term of (20) to include the interval $|s-s'|<\Delta s$, which introduces a small error of order Ka but removes from consideration the arbitrary parameter Δs subject to the assumption $a\ll\Delta s\ll c_{wire}^{-1}$. Substituting the result into (9) we find:

$$\int\left(i\pi K_p^2e^{ips}H_0^{(1)}(K_pa)J_0(K_pa)+K^3\int V(s,s')e^{ips'}ds'\right)j_pdp= \qquad (23)$$
$$=i4\pi\varepsilon_0\omega\vec{E}^{(in)}(\vec{r}_s)\frac{d\vec{r}_s}{ds}.$$

Substituting into (23) the expression for $\hat{j}_p$ by inverting (8):

$$j_p=\frac{1}{2\pi}\int_{-\infty}^{\infty}e^{-ips}j_sds$$

and integrating over p we obtain the following equation:

$$\left(K^2+\frac{d^2}{ds^2}\right)\int_{-L/2}^{L/2}T(s-s')j_{s'}ds'+K^3\int_{-L/2}^{L/2}V(s,s')j_{s'}ds'= \qquad (24)$$
$$=i4\pi\varepsilon_0\omega\vec{E}^{(in)}(\vec{r}_s)\frac{d\vec{r}_s}{ds},$$

where L is the antenna length and

$$T(s)=\frac{i}{2}\int_{-\infty}^{\infty}H_0^{(1)}\left(\sqrt{K^2-p^2}a\right)J_0\left(\sqrt{K^2-p^2}a\right)e^{ips}dp. \qquad (25)$$

In fact, $T(s)$ in (24) coincides with the so-called "exact" kernel of the Pocklington equation [1,2]. To verify this one can repeat the steps that led to representation (25) in reverse order, that is, replace the product of $H_0^{(1)}$ and J_0 in (25) by the LHS of (18), and then use representation (17). The integration over p then produces a δ-function and one obtains:

$$T(s)=\frac{1}{2\pi}\int_{-\infty}^{\infty}\frac{e^{iK\sqrt{s^2+4a^2\sin^2(\theta/2)}}}{\sqrt{s^2+4a^2\sin^2(\theta/2)}}d\theta. \tag{26}$$

The asymptotic form of the Bessel functions in (25), which takes into account that generally $K_p a \ll 1$, can also be used if preferable. In particular, expanding in (26) $J_0(K_p a)$ into a power series one obtains:

$$T(s)=\sum_{n=0}^{\infty}(-1)^n\frac{a^{2n}\left(K^2+\frac{d^2}{ds^2}\right)^n}{2^{2n}(n!)^2}\frac{i}{2}\int_{-\infty}^{\infty}H_0^{(1)}\left(\sqrt{K^2-p^2}\,a\right)e^{ips}dp$$

or, after calculating the integral using formula 6.677(8) in [15]:

$$T(s)=\sum_{n=0}^{\infty}(-1)^n\frac{a^{2n}\left(K^2+\frac{d^2}{ds^2}\right)^n}{2^{2n}(n!)^2}\frac{e^{iK\sqrt{a^2+s^2}}}{\sqrt{a^2+s^2}}. \tag{27}$$

The first term $n=0$ in (27) corresponds to the so-called "approximate" kernel, and the rest of the sum represents corrections that are generally of order $(aK)^{2n}$ (a similar representation was considered in [16]).

Equations (23) and (24) are the major results of this work. It is easy to show that for a straight wire the kernel V becomes zero, and (24) coincides with the Pocklington equation. For the case of a curved wire, (24) includes an additional integral term. An important difference with respect to previously considered formulations for curved wires [10-12] is that the integral V-term in (24), which represents the effects of the deviation of the wire from a straight segment, does not depend on the wire's radius and has a non-singular kernel.

III. The Case of a Loop Wire

Let us assume that the wire forms a closed loop of length L (not necessarily circular, or a single turn, or of trivial topology [17]). In this case it is convenient to start with (23) in which we can now set

$$j_p=\sum_{m=-\infty}^{\infty}j_m\delta\left(p-\frac{2\pi}{L}m\right). \tag{28}$$

For the case of a loop wire, however, we have to make in (23) the modification mentioned in the paragraph following (21), namely, since now the integration over s' in the second integral term in (19) is limited to $(-L/2, L/2)$, in the RHS of (19) there now appears an additional term $exp(i2\pi ms/L)\,K^2\tilde{v}_m$, where

$$\begin{aligned}\tilde{v}_m&=\frac{1}{K^2}\int_{|t|>L/2}^{\infty}\left(-\frac{2}{|t|^3}+\frac{2iK}{t^2}\right)e^{iK|t|+i2\pi m/Lt}dt=\\&=4(-1)^m\frac{iKL-2}{(KL)^2}e^{iKL/2}-\frac{K_m^2}{K^2}Ei\big(i(KL/2+\pi m)\big)-\\&\qquad-\frac{K_m^2}{K^2}Ei\big(i(KL/2-\pi m)\big).\end{aligned} \tag{29}$$

In (29), and in what follows,

$$K_m=\sqrt{K^2-\left(\frac{2\pi}{L}m\right)^2},\ \mathrm{Im}\,K_m\ge 0 \tag{30}$$

and

$$Ei(ix)=\int_1^{\infty}\frac{e^{ixt}}{t}dt \tag{31}$$

is the exponential integral function of imaginary argument. Substituting (28) into (23), taking into account (29), multiplying by $exp(-i2\pi ns/L)/(K^2L)$, and integrating over s, one obtains the following governing equation:

$$\begin{aligned}&\left(i\pi\frac{K_n^2}{K}H_0^{(1)}(K_n a)J_0(K_n a)+\tilde{v}_n\right)j_n+\sum_{m=-\infty}^{\infty}V_{nm}j_m=\\&\qquad=i\frac{4\pi\varepsilon_0\omega}{K^2L}\int_{-L/2}^{L/2}e^{-i2\pi ns/Ls}\vec{E}^{(in)}(\vec{r}_s)\frac{d\vec{r}_s}{ds}ds,\end{aligned} \tag{32}$$

where

$$V_{nm}=\frac{K}{L}\int_{-L/2}^{L/2}\int_{-L/2}^{L/2}V(s,s')e^{-i\frac{2\pi}{L}(ns-ms')}ds\,ds' \tag{33}$$

and the regular dimensionless function $V(s,s')$ in (33) is given by (21). In fact, one can set in (32) $J_0(K_n a)=1$.

For numerical simulations let us consider the case of a circular wire loop of radius ρ. In this case

$$V(s,s')=V^{(c)}(\rho,|\theta-\theta'|), \tag{34}$$

where $\theta=s/\rho$ is an azimuthal angle. Then one obtains $V_{nm}=V_n^{(c)}\delta_{nm}$, where

$$V_n^{(c)}=2K\rho\int_0^{\pi}V^{(c)}(\rho,\theta)\cos n\theta\,d\theta$$

and (32) provides an explicit result:

$$\begin{aligned}j_n=i\frac{\omega}{K^2L}&\left(i\pi\frac{K_n^2}{K^2}e^{ips}H_0^{(1)}(K_n a)J_0(K_n a)+\tilde{v}_n+V_n^{(c)}\right)^{-1}\times\\&\times\int_{-L/2}^{L/2}\vec{E}^{(in)}(\vec{r}_s)\frac{d\vec{r}_s}{ds}e^{-in\frac{2\pi}{L}s}ds.\end{aligned} \tag{35}$$

Let us consider the case of a plane wave propagating along the z-axis orthogonal to a circular loop lying in the (x,y) plane centered at the origin, with an incident electric field vector directed along x-axis of amplitude E_0. Then, in the RHS of (32), one has

$$\vec{E}^{(in)}(\vec{r}_s)\frac{d\vec{r}_s}{ds} = E_0\cos\theta,$$

and the integral in the RHS of (32) is nonzero for $n = \pm 1$ only, that is, the induced current is a sinusoidal function of the arclength. The results of a numerical calculation of the x-component of the total electric field (i.e., the sum of the incident and scattered fields) as a function of y-coordinate is shown in Fig.2. The radius of the circular loop was set to ρ=1 m, the wavelength to λ=2 m, and radius of the wire to a=1 mm. The electric field was calculated by direct numerical integration (using Simpson's rule) of the 3D integral in (2), with $j_{\pm 1}$ given by (35). The total electric field (Fig. 2, upper plot) tends to zero at the surface of the wire as it should. An enlarged section of the plot in the vicinity of the wire is shown in the lower figure. One can see that at distances too close to the wire direct numerical integration begins to lose accuracy. It is worth mentioning that the second term $V_1^{(c)}$ in the denominator of (35), which takes into account the curvature of the loop, constitutes about 10.6 % of the first term.

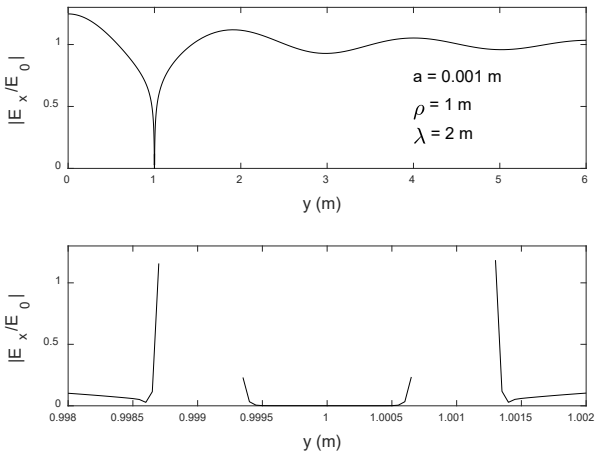

Fig. 2: The total normalized electric field amplitude $|E_x/E_0|$ as a function of the y-coordinate for a circular loop antenna centered on the x-y plane and a normally incident plane wave with an x-directed electric field of magnitude E_0. The total field tends to zero at the surface of the wire. The lower plot is an enlarged version of the upper plot in the vicinity of the wire. The artificial rise in the intensity is due to the loss of the accuracy of the direct numerical integration in (2) when the observation point gets too close to the wire surface. This reflects the fact that direct setting of the observation point onto the surface of the wire leads to divergent integrals.

We have also considered the case of delta-gap excitation of the loop assuming

$$\vec{E}^{(in)}(\vec{r}_s) = V_0\delta(\rho\theta)\vec{e}_y$$

In Fig. 3 we show the amplitudes of the harmonics $\hat{j}_n$ of the induced current in the upper plot, and the resulting current $I = \Sigma\hat{j}_n$ in the lower plot. The voltage was set to V_0 = 1 V.

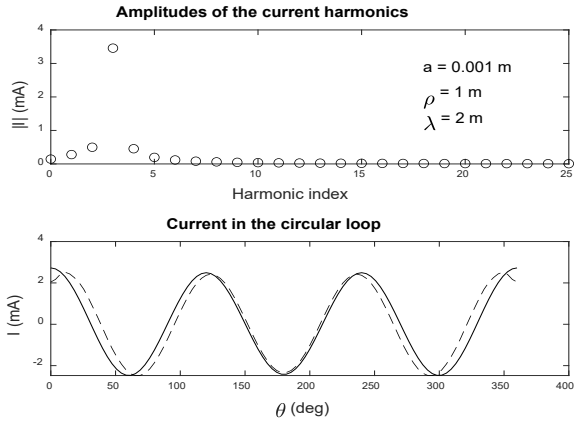

Fig.3: The upper figure shows the amplitudes of the harmonics of the induced current I as a function of the harmonic index for a δ-gap loop antenna and the geometry described in Fig. 2. The lower figure shows the real and imaginary parts of the resulting current (solid and dashed lines, respectively) as a function of azimuthal angle θ.

The dependence of the input admittance of the loop, which is defined as a ratio of the induced current at the point of excitation $(\rho, 0)$ to the voltage V_0, is shown in Fig. 4 as a function of the ratio of the loop diameter 2ρ to the wavelength. The circles represent the theoretical results presented in Storer (eq.(10) in [18]), and the solid/dashed lines the theory presented here for the real/imaginary parts of the input admittance. The agreement is good with the exception of a slight deviation of the imaginary part of the admittance for relatively small loops. A possible reason for this may be the additional approximations introduced in [18] to evaluate analytically certain integrals that here were calculated by direct numerical integration.

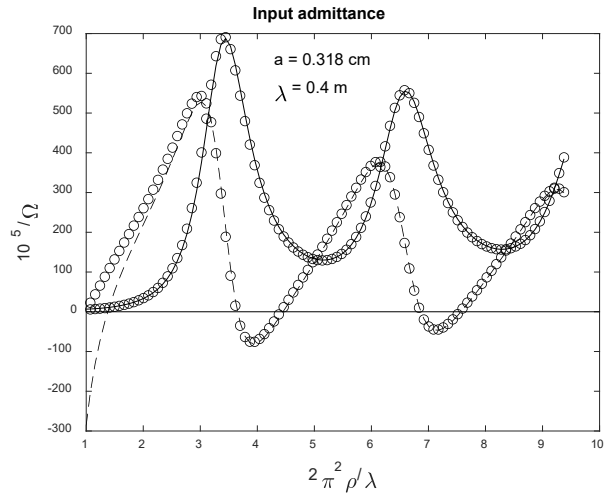

Fig. 4. The theoretical input admittance of the circular loop wire antenna for the geometry described in Fig. 2 calculated from eq. (35) with a δ-gap excitation as a function of the normalized loop diameter $2\rho\pi^2/\lambda$. Both the real- and imaginary parts of the impedance (solid and dashed lines, respectively) are shown. The circles indicate theoretical results reproduced according to eq. (10) in [18].

A comparison between our theoretical result for the input admittance and the measured input admittance from Kennedy [19] is shown in Fig. 5. The latter was generated by digitizing Fig. 11 in [19]. The agreement is exceptionally good for the real part and deviates only slightly for the imaginary part.

Together, Figures 4 and 5 demonstrate the relatively good agreement between the new theory developed here and earlier theoretical developments and measurement campaigns. As was mentioned before, the function V in (21) and (34) is in fact non-singular. A non-singular analytic form of the function $V(s,s')$ for a circular loop is presented for reference purposes in Appendix A.

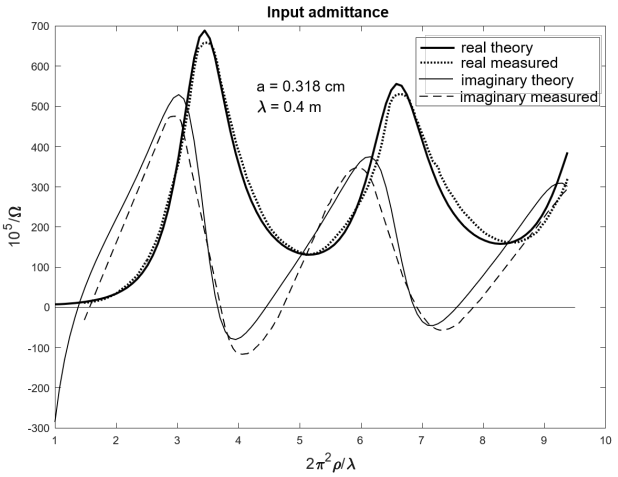

Fig. 5. The theoretical input admittance of the circular loop wire antenna for the geometry described in Fig. 2 calculated from eq. (35) with a δ-gap excitation as a function of the normalized loop diameter $2\rho\pi^2/\lambda$ compared with the measured results of Kennedy [19]. Both the real- and imaginary parts of the admittance (solid and dashed lines, respectively) are shown.

IV. The Case of an Open-Ended Wire

For the case of open-ended wire, the governing equation (24) coincides with the standard Pocklington equation with an additional integral term having a non-singular kernel. Thus, all methods developed for numerical solution of the Pocklington equation can be applied to (24) with a straightforward modification.

The first and the second integral terms in (24) are significantly different. Namely, the kernel V of the second term represents a non-singular function and can be calculated by any suitable integration scheme (e.g., by the Simpson's rule) with a grid of points with a density that is not related to wire radius a. The first integral in (24), on the other hand, has a logarithmic singularity at $s'=s$, and in the vicinity of this point varies on the scale of the wire radius a. This logarithmic singularity ensures that the Pocklington equation for a straight wire with the exact kernel is solvable [3], and special care must be taken to account for this singularity in the numerical simulations. In this Section we suggest an alternative approximate form of the Pocklington equation that does not have such a problem. In this form a wire radius a enters the governing equation only in diagonal elements of the interaction matrix.

In what follows it will be more convenient to replace the limits of integration in (24) by $(0,L)$, and represent the current in the form

$$j_s=\sum_{m=1}^{\infty} j_m \sin(\xi_m s),\quad \xi_m=m\frac{\pi}{L}\,. \tag{36}$$

This representation ensures fulfillment of the boundary conditions $j(0)=j(L)=0$. Let us substitute (36) into (24), represent $d^2/ds^2T(s-s')=-d^2/dsdsT(s-s')$, multiply the result by $2\sin(\xi_n L)/(K^2L)$, and integrate by parts transferring the action of the differential operators from the kernel T to the *sin*-functions. As a result, one obtains:

$$\sum_{m=1}^{\infty}\left(T_{nm}^{(S)}-\frac{\xi_n\xi_m}{K^2}T_{nm}^{(C)}+V_{nm}\right)j_m=i\frac{8\pi\varepsilon_0\omega}{LK^2}\int_0^L\sin(\xi_n s)\vec{E}^{(in)}(\vec{r}_s)\frac{d\vec{r}_s}{ds}ds \tag{37}$$

where

$$T_{nm}^{(S)}=\frac{2}{L}\int_0^L ds\sin(\xi_n s)\int_0^L T(s-s')\sin(\xi_m s')ds', \tag{38}$$

$$T_{nm}^{(C)}=\frac{2}{L}\int_0^L ds\cos(\xi_n s)\int_0^L T(s-s')\cos(\xi_m s')ds', \tag{39}$$

and

$$V_{nm}=2\frac{K}{L}\int_0^L ds\sin(\xi_n s)\int_0^L V(s,s')\sin(\xi_m s')ds'.$$

Expressing (24) in terms of the functions $\sin(\xi_n L)$ somewhat restricts the class of the RHS of (24), however, it simplifies the results. To maintain similarity with the case of loop wires we will represent (37) in the following form:

$$\begin{aligned}i\pi\frac{K_n^2}{K^2}H_0^{(1)}(K_n a)j_n+\sum_{m=1}^{\infty}(T_{nm}+V_{nm})j_m=\\ =i\frac{8\pi\varepsilon_0\omega}{LK^2}\int_0^L\sin(\xi_n s)\vec{E}^{(in)}(\vec{r}_s)\frac{d\vec{r}_s}{ds}ds,\end{aligned} \tag{40}$$

where

$$T_{nm}=T_{nm}^{(S)}-\frac{\xi_n\xi_m}{K^2}T_{nm}^{(C)}-i\pi\frac{K_n^2}{K^2}H_0^{(1)}(K_n a)\delta_{nm}. \tag{41}$$

The last term in (41) will be compensated by corresponding contributions in $T_{nm}^{(S)}$, $T_{nm}^{(C)}$ so that T_{nm} in the LHS of (41) is in fact independent on wire radius a. The procedure for the calculation of entries T_{nm} is presented in Appendix B. For straight wires one has in (40) $V_{nm}=0$.

The results of a case study of (40) are shown on Fig. 6. A standing plane wave impinges on a piece of straight wire of length L = 2.25 m at an angle 30° so that

$$\vec{E}^{(in)}(\vec{r}_s)\frac{d\vec{r}_s}{ds}=E_0\cos\left(\frac{K}{2}\left(s-\frac{L}{2}\right)\right).$$

The wavelength is λ = 1 m and the wire radius is a = 1 mm. The incident field is distributed along the wire length symmetrically so that only modes with odd indices m in (36) are excited. Twenty odd modes were included into the numerical solution of (40). The amplitudes of the excited modes as a function of mode index are shown on the upper plot

of Fig. 6 (only odd modes are shown and the strength of the electric field was set to E_0 = 1 V/m). The dependence of the total electric field as a function of *y*-coordinate (which is orthogonal to the plane of incidence) is shown on the lower plot (which is similar to Fig. 2). The total electric field at the wire tends to zero confirming the validity of the obtained solution.

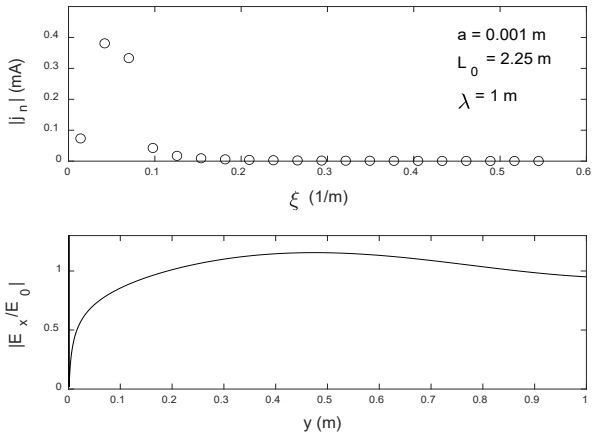

Fig. 6. The mode amplitude $|j_n|$ as a function of mode index ξ (top) and the total normalized electric field amplitude $|E_x/E_0|$ as a function of the *y*-coordinate (bottom) for a straight wire antenna centered on the *x*-*y* plane and a plane wave of amplitude E_0 normally incident at an azimuthal angle of 30°.

V. The Case of a Sectioned Wire

The case of a single-piece wire was so far considered in this work. However, generalization of the governing equation for the case of an antenna consisting of multiple pieces is straightforward. Eq. (24) in this case takes the following form:

$$\left(K^2+\frac{d^2}{ds^2}\right)\int_{-L_q/2}^{L_q/2} T(s-s')\,j_{s'}^{(q)}ds' + K^3\sum_{q'=1}^{Q}\int_{-L_{q'}/2}^{L_{q'}/2} V_{qq'}(s,s')\,j_{s'}^{(q')}ds' = i4\pi\varepsilon_0\omega\vec{E}^{(in)}\left(\vec{r}_s^{(q)}\right)\frac{d\vec{r}_s^{(q)}}{ds} \quad (42)$$

where $q=1,2,\ldots,Q$ is an index representing different pieces of the wire, and

$$V_{qq'}(s,s') = \left(-\frac{2}{K^3|s'-s|^3}+\frac{2i}{K^2(s'-s)^2}\right)e^{iK|s'-s|}\delta_{qq'} + \frac{1}{K^3}U_{qq'}(s,s'), \quad (43)$$

where

$$U_{qq'}(s,s') = \frac{e^{iKr}}{r^3}\left[\begin{array}{l}\left(K^2r^2+iKr-1\right)\left(\frac{d\vec{r}_s^{(q)}}{ds},\frac{d\vec{r}_{s'}^{(q')}}{ds'}\right)- \\ -\left(K^2r^2+3iKr-3\right)\times \\ \times\left(\frac{\vec{r}_s^{(q)}-\vec{r}_{s'}^{(q')}}{r},\frac{d\vec{r}_s^{(q)}}{ds}\right)\left(\frac{\vec{r}_s^{(q)}-\vec{r}_{s'}^{(q')}}{r},\frac{d\vec{r}_{s'}^{(q')}}{ds'}\right)\end{array}\right], \quad (44)$$

where the bracketed term is evaluated at $r=\left|\vec{r}_s^{(q)}-\vec{r}_{s'}^{(q')}\right|$. Clearly $U_{qq'}(s,s')=U_{q'q}(s',s)$ and $V_{qq'}(s,s')$ are non-singular functions.

VI. Discussion and Conclusions

In this work the Pocklington equation for a thin, bent, ideally conducting wire was derived in a special form where the integral term, which represents curvature effects, has a non-singular kernel independent on wire radius (see (24)). To the best of authors' knowledge such a form of the Pocklington equation was not considered in the literature previously.

For loop wires the derived equation can be conveniently formulated in terms of the Fourier-harmonics of the current (see (32)). Numerical simulations for a circular wire confirm fulfillment of the boundary condition. A similar equation was derived for the open-ended wires (see (37) and also for sectioned wires (see (42)).

It was mentioned before that the wire is not required to be single-turn and can generally have an arbitrary shape. However, for the case of multiple turns/recurrences it is assumed that different turns are not too close to each other. When deriving the basic equations (23) and (24) it was assumed that the distance between the points separated by the arclength exceeding $\Delta s \gg a$ are "far" points, that is, the distance between a given point and all other points on the wire beyond Δs significantly exceeds a. Hence, the separation between corresponding points of the wire for different turns should significantly exceed radius of the wire.

Appendix A

Let us set in (7) $s'=s+t$ where $t>0$ and $t\to+0$. One has:

$$\vec{r}_{s+t}-\vec{r}_s = t\partial_s\vec{r}+\frac{t^2}{2}\partial_s^2\vec{r}+\frac{t^3}{6}\partial_s^3\vec{r}+O\left(t^4\right). \quad (A1)$$

By differentiating the identity $(\partial_s\vec{r},\partial_s\vec{r})=1$ one has $(\partial_s\vec{r},\partial_s^2\vec{r})=0$, and differentiating the latter identity one more time one finds $(\partial_s\vec{r},\partial_s^3\vec{r})=-(\partial_s^2\vec{r})^2$. Using these identities, one obtains:

$$r^2=\left|\vec{r}_{s+t}-\vec{r}_s\right|^2=t^2-\alpha t^4+O\left(t^5\right),$$
$$r=t\left(1-\frac{\alpha}{2}t^2\right)+O\left(t^4\right), \quad (A2)$$

where

$$\alpha=\frac{1}{12}\left(\partial_s^2\vec{r}\right)^2.$$

Using (A2) one can also represent (A1) in the following form:

$$\vec{r}_{s+t}-\vec{r}_s = r\partial_s\vec{r}+\frac{r^2}{2}\partial_s^2\vec{r}+\left(\frac{\alpha}{2}\partial_s\vec{r}+\frac{1}{6}\partial_s^3\vec{r}\right)r^3+O\left(r^4\right).$$

Now by straightforward calculations one obtains the following expansions:

$$\frac{d\vec{r}_{s'}}{ds'}=\partial_s\vec{r}+t\partial_s^2\vec{r}+\frac{t^2}{2}\partial_s^3\vec{r}+O\left(t^3\right),$$
$$\left(\frac{d\vec{r}_{s'}}{ds'},\frac{d\vec{r}_s}{ds}\right)=1-6\alpha r^2+O\left(r^3\right),$$
$$\left(\frac{\vec{r}_{s+t}-\vec{r}_s}{r},\frac{d\vec{r}_{s'}}{ds'}\right)=\left(\frac{\vec{r}_{s+t}-\vec{r}_s}{r},\frac{d\vec{r}_s}{ds}\right)=1-\frac{3}{2}\alpha r^2+O\left(r^3\right).$$

Using these expansions, one obtains:

$$U\left(s+t,s\right)=\frac{e^{iKr}}{r^3}\left[\left(K^2r^2+iKr-1\right)\left(1-6ar^2\right)-\left(K^2r^2+3iKr-3\right)\times\right.$$
$$\left.\times\left(1-\frac{3}{2}ar^2\right)^2+O\left(r^3\right)\right]=e^{iKr}\left(\frac{2}{r^3}-\frac{2iK}{r^2}-\frac{3\alpha}{r}\right)+O(1)$$

and then using (A2):

$$U\left(s+t,s\right)=e^{iKt}\left(\frac{2}{t^3\left(1-\frac{\alpha}{2}t^2\right)^3}-\frac{2iK}{t^2}-\frac{3\alpha}{t}\right)+O(1)=$$
$$=e^{iKt}\left(\frac{2}{t^3}-\frac{2iK}{t^2}\right)+O(1).$$

Quite similarly one considers the case of negative t: $t\to-0$. In the latter case parameter t in the resulting formula has to be replaced by $|t|$. It is interesting that parameter α associated with curvature of the central line disappears from the final formula for $U(s+t,s)$. One can see that the first two (singular) terms in (21) cancel out by corresponding terms in U.

Let us consider the case of a circle with radius ρ and let $\theta>0$ is an angle between s and s' points on the circle. In this case

$$\left|s'-s\right|=\rho\theta,\quad r=2\rho\sin\frac{\theta}{2}$$

and

$$V\left(\theta\right)=\left(-\frac{2}{K^3\rho^3\theta^3}+\frac{2i}{K^2\rho^2\theta^2}\right)e^{iK\rho\theta}+\frac{e^{iK\rho\sin(\theta/2)}}{K^3\rho^3\sin^3\left(\theta/2\right)}\times$$
$$\times\left\{\left[K^2\rho^2\sin^2\left(\theta/2\right)+iK\rho\sin\left(\theta/2\right)-1\right]\cos\theta-\right.$$
$$\left.-\left[K^2\rho^2\sin^2\left(\theta/2\right)+3iK\rho\sin\left(\theta/2\right)-3\right]\cos^2\left(\theta/2\right)\right\}\qquad\text{(A3)}$$

A non-singular expression for V can be represented as follows. Let us define a function:

$$\gamma\left(\theta\right)=\begin{cases}\dfrac{2\sin\frac{\theta}{2}-\theta+\frac{\theta^3}{24}}{\theta^5}, & \theta>\delta\\ \displaystyle\sum_{n=2}^{\infty}\frac{\left(-1\right)^n\theta^{2n-4}}{2^{2n}\left(2n+1\right)!}, & \theta<\delta\end{cases}.$$

In our numerical simulations we selected $\delta=0.25$. Let us also introduce the following parameters:

$$\beta_1=-\frac{1}{24}+\gamma\left(\theta\right)\theta^2,$$
$$\beta_2=\beta_1\theta^2,$$
$$\beta_3=K\rho\beta_1\theta^3,$$

and values

$$M_1=2-4K^2\rho^2\sin^4\frac{\theta}{2}+\sin^2\frac{\theta}{2}\left(2iK\rho\sin\frac{\theta}{2}-1\right)-4iK\rho\sin\frac{\theta}{2},$$
$$M_2=-\frac{2}{K^3\rho^3\left(1+\beta_2\right)^3}\left[3\theta\gamma\left(\theta\right)\left(1+\beta_2\right)^2-\theta\beta_1^2\left(3+2\beta_2\right)-\right.$$
$$\left.-iK\rho\beta_1\left(2+\beta_2\right)\left(1+\beta_2\right)\right].$$

Then

$$V\left(\theta\right)=e^{iK\rho\theta}\left[ie^{i\beta_3/2}\left(1-\beta_3^2\left(\frac{1}{24}-\beta_3^2\gamma\left(\beta_3\right)\right)\right)\frac{\beta_1M_1}{K^2\rho^2\left(1+\beta_2\right)^3}-\right.\qquad\text{(A4)}$$
$$\left.-\frac{\sin\left(\theta/2\right)}{2K\rho}+\frac{i}{4K^2\rho^2}+M_2\right]$$

The easiest way to make sure that representations (A3) and (A4) in fact coincide is to do this numerically for not too small values of θ, when (A3) due to cancellation of singularities starts to lose accuracy.

APPENDIX B

Let us calculate the following function:

$$B\left(\xi_n,\xi_m\right)=\frac{1}{L}\int_{-L/2}^{L/2}ds e^{-i\xi_n s}\int_{-L/2}^{L/2}T\left(s-s'\right)e^{i\xi_m s'}ds'\qquad\text{(B1)}$$

where ξ_n,ξ_m are considered as real parameters which in contrast to (36) here can have arbitrary sign (it is convenient at this point to set integration limits to $(-L/2,L/2)$). In terms of functions $B\left(\xi_n,\xi_m\right)$ one has:

$$T_{nm}^{(S)}=\frac{1}{2}\begin{pmatrix}e^{-i\left(\xi_n-\xi_m\right)\frac{L}{2}}B\left(\xi_n,\xi_m\right)+e^{i\left(\xi_n-\xi_m\right)\frac{L}{2}}B\left(-\xi_n,-\xi_m\right)-\\ -e^{i\left(\xi_n+\xi_m\right)\frac{L}{2}}B\left(-\xi_n,\xi_m\right)-e^{-i\left(\xi_n+\xi_m\right)\frac{L}{2}}B\left(\xi_n,-\xi_m\right)\end{pmatrix},\qquad\text{(B2a)}$$

$$T_{nm}^{(C)}=\frac{1}{2}\begin{pmatrix} e^{-i(\xi_n-\xi_m)\frac{L}{2}}B(\xi_n,\xi_m)+e^{i(\xi_n-\xi_m)\frac{L}{2}}B(-\xi_n,-\xi_m)+ \\ +e^{i(\xi_n+\xi_m)\frac{L}{2}}B(-\xi_n,\xi_m)+e^{-i(\xi_n+\xi_m)\frac{L}{2}}B(\xi_n,-\xi_m) \end{pmatrix}. \qquad \text{(B2b)}$$

Let us introduce on the complex p-plane in (25) two cuts that are parallel to the imaginary axis and pass from point $p=-K-i\varepsilon$ toward $-i\infty$ and from point $p=K+i\varepsilon$ toward $+i\infty$; it is thus assumed that K has a small positive imaginary part: $\varepsilon\to+0$. Such selection of cuts ensures that the imaginary part of K_p in (14) (the argument of the cylindrical functions in (25)) is always positive.

We substitute into the (B1) representation (25) and integrate over s' first:

$$\int_{-L/2}^{L/2}T(s-s')e^{i\xi_m s'}ds'= \\ =\frac{i}{2}\int_{-\infty}^{\infty}H_0^{(1)}(K_pa)J_0(K_pa)e^{ips}\frac{e^{i(p-\xi_m)L/2}-e^{-i(p-\xi_m)L/2}}{i(p-\xi_m)}dp, \qquad \text{(B3)}$$

where K_p is given by (14). We will assume that the original integration path with respect to p in (25), which goes along real axis, was shifted slightly downwards. Now we represent the RHS of (B3) as a sum of two integrals associated with the first- and the second exponential. The integration path in the first term will be moved to the upper half-plane of p; it will be encompassing the cut coming from point $p=K+i\varepsilon$ to $+i\infty$; let us denote this contour as C_+. In the process of the path deformation the pole at $p=\xi_m$ in (B3) is apparently crossed, and corresponding residue must be added to the result. It is easy to see from (14) that the argument of K_p at the right edge of the cut as compared to the left edge increases by π and the integration path goes in the opposite direction. Thus, one finds:

$$\int_{C_+}H_0^{(1)}(K_pa)J_0(K_pa)\frac{e^{ip(s+L/2)}}{p-\xi_m}dp= \\ =\int_{C_+^{(left)}}\left(H_0^{(1)}(K_pa)-H_0^{(1)}(e^{i\pi}K_pa)\right)J_0(K_pa)\frac{e^{ip(s+L/2)}}{p-\xi_m}dp$$

Since $H_0^{(1)}(e^{i\pi}z)=-H_0^{(2)}(z)$ (see [15], eq. 8.476(8)) one finds:

$$\int_{C_+}H_0^{(1)}(K_pa)J_0(K_pa)\frac{e^{ip(s+L/2)}}{p-\xi_m}dp= \\ =2\int_{C_+^{(left)}}J_0^2(K_pa)\frac{e^{ip(s+L/2)}}{p-\xi_m}dp \qquad \text{(B4)}$$

The Bessel function in the integrand of the RHS of (B4) grows for large $p''=Im\,p>0$ as $exp(2ap'')$, however this growth is compensated by the exponential which decays as $exp(-(s+L/2)p'')$. Thus, the integral actually diverges for the points s which are closer to the left end of the wire than $2a$, and converges otherwise. Neglecting the effects of wire ends, which are not accurately accounted for in this approach anyway, we will set in (B4) $J_0(K_pa)\approx 1$. This approximation restricts the maximal index of modes that may be included into analysis, that is, they have to satisfy

$$|K_n|a<<1.$$

The second integral in (B3) is analyzed quite similarly. This time the integration path is moved down and encompasses the cut in the lower half-space of p denoted as C_-. The only difference with the previous case is that now the pole at $p=\xi_m$ when moving integration path is not crossed. As a result, one obtains:

$$\int_{-L/2}^{L/2}T(s-s')e^{i\xi_m s'}ds'=i\pi e^{i\xi_m s}H_0^{(1)}(K_ma)+ \\ +e^{-i\xi_m L/2}\int_{C_+^{(left)}}^{\infty}\frac{e^{ip(s+L/2)}}{p-\xi_m}dp-e^{i\xi_m L/2}\int_{C_-^{(right)}}^{\infty}\frac{e^{ip(s-L/2)}}{p-\xi_m}dp. \qquad \text{(B5)}$$

Now we multiply equation (B5) by $L^{-1}exp(-i\xi_n s)$ and integrate over s. Straightforward calculations give the following result:

$$B(\xi_n,\xi_m)=i\pi H_0^{(1)}(K_na)\delta(\xi_n-\xi_m)+W(\xi_n,\xi_m)+W(-\xi_m,-\xi_n), \qquad \text{(B6)}$$

where $\delta(\xi_n-\xi_m)=1$ if $\xi_n=\xi_m$ and is zero otherwise, and

$$W(\xi_n,\xi_m)=\frac{1}{L}\int_0^{\infty}\frac{e^{-i(\xi_n-\xi_m)L/2}-e^{i(\xi_n+\xi_m)L/2}e^{i(K+it)L}}{(K+\xi_n+it)(K+\xi_m+it)}dt. \qquad \text{(B7)}$$

The explicit expression for $W(\xi_n,\xi_m)$ can be easily worked out and is as follows. For $\xi_n\neq\xi_m$ one has:

$$W(\xi_n,\xi_m)=i\frac{e^{-i(\xi_n-\xi_m)L/2}}{(\xi_n-\xi_m)L}\left[-\log\left|\frac{K+\xi_n}{K+\xi_m}\right|+i\frac{\pi}{2}sign(K+\xi_n)- \right. \\ \left. -i\frac{\pi}{2}sign(K+\xi_m)-Ei(i(K+\xi_n)L)+e^{i(\xi_n-\xi_m)L}Ei(i(K+\xi_m)L)\right] \qquad \text{(B8)}$$

and, for $\xi_n=\xi_m$:

$$W(\xi_n,\xi_n)=-i\frac{1-e^{i(K+\xi_n)L}}{(K+\xi_n)L}-Ei(i(K+\xi_n)L). \qquad \text{(B9)}$$

Now substituting (B6) into (B2) and then into (41) one obtains the expression for the interaction matrix T_{nm} in (40). Note, that the terms proportional to $H_0^{(1)}(K_na)$ in (41) cancel out, and the expression for T_{nm} includes only W-terms given by (B8), (B9) and thus are non-singular and do not depend on wire radius a.

ACKNOWLEDGEMENTS

The authors would like to acknowledge the many helpful comments and recommendations of the reviewers. They helped to improve the clarity of a very detailed development. The authors would also like to thank the NOAA Physical Sciences Laboratory for its support of this work.

REFERENCES

[1] J. Jackson, "*Classical Electrodynamics*", 3rd ed., Wiley, 1999.

[2] C.A. Balanis "*Antenna Theory, Analysis and Design*", 4th ed., Wiley, 2016.

[3] D. Jones, "Note on the integral equation for a straight wire antenna", Proc. IEE, v. 128(H), No. 2, pp. 114-116, 1981.

[4] B. Rynne, "On the well-posedness of Pocklington's equation for a straight wire antenna and convergence of numerical solutions", J. Electromagn. Waves Application, v. 14, pp. 1489–1503, 2000.

[5] G. Fikioris, "The approximate integral equation for a cylindrical scatterer has no solution", J. Electromagn. Waves Application, v. 15 (9), pp. 1153–1159, 2001.

[6] J. Papakanellos, G. Fikioris, and A. Michalopoulou, "The oscillations appearing in numerical solutions of solvable and non-solvable integral equations for thin-wire antennas", IEEE Trans. Antennas Prop., v. 58 (5), pp. 1635-1644, 2010.

[7] P. Davies, D. Duncan and S. Funken, "Accurate and efficient algorithms for frequency domain scattering from a thin wire", J. of Computational Physics, v. 168 (1) pp. 155-183, 2001.

[8] G. Fikioris and T. T. Wu, "On the application of numerical methods to Hallen's equation", IEEE Trans. Antennas Propag., vol. 49, no. 3, pp. 383–392, 2001.

[9] D. Werner, J. Huffman, and P. Werner, "Techniques for evaluating the uniform current vector potential at the isolated singularity of the cylindrical wire kernel", IEEE Trans. Antennas Prop., v. 42 (11), pp. 1549-1553, (1994).

[10] C. Tang, "Input impedance of arc antennas and short Helical radiators", IEEE Trans. Antennas Prop., AP-12 (1), pp. 2-9, 1964.

[11] K.K. Mei "On the integral equations of thin wire antennas", IEEE Trans. Antennas Prop., AP-13 (3), pp. 374-378, 1965.

[12] H. Nakano, "The integral equations for a system composed of many arbitrary bent wires", The Transactions of the IECE of Japan, v. E65 (6), pp. 303-309, 1982.

[13] E. Rothwell and N. Gharsallah, "Determination of the natural frequencies of a thin wire elliptical loop", IEEE Trans. Antennas Prop., v. 35 (11), pp. 1319-1324, 1987.

[14] S. Eminov and A. Sochilin "A numerical-analytic method for solving integral equations of dipole antennas", J. of Communications Technology and Electronics, v. 62 (1), pp. 55-60, 2017.

[15] I.S. Gradshteyn and I.M. Ryzhik, *"Tables of Integrals, Series, and Products"*, Fifth Ed., Academic Press, 1965.

[16] D. Werner, "An exact formulation for the vector potential of a cylindrical-antenna with uniformly distributed current and arbitrary radius", IEEE Trans. Antennas Prop., v. 41 (8), pp. 1009-1018, 1993.

[17] D. Werner, "Radiation and scattering from thin toroidally knotted wires", IEEE Trans. Antennas Prop., v. 47 (8), pp. 1351-1363, 1999.

[18] J. Storer, "Impedance of thin-wire loop antennas", Proc. AIEE, pp. 606-619, 1956.

[19] P. Kennedy, "Loop antenna measurements," IRE Transactions on Antennas and Propagation, vol. 4, no. 4, pp. 610-618, 1956.